

See discussions, stats, and author profiles for this publication at: <https://www.researchgate.net/publication/256295581>

Photoenhanced Degradation of Methylene Blue on Cospattered M:TiO₂ (M = Au, Ag, Cu) Nanocomposite Systems: A Comparative Study

ARTICLE *in* THE JOURNAL OF PHYSICAL CHEMISTRY C · JUNE 2010

Impact Factor: 4.77 · DOI: 10.1021/jp910454r

CITATIONS

69

READS

260

3 AUTHORS, INCLUDING:



Parvah Sangpour

Materials and Energy Research Center

26 PUBLICATIONS 319 CITATIONS

[SEE PROFILE](#)



Fatemeh Sadat Minaye Hashemi

Stanford University

7 PUBLICATIONS 108 CITATIONS

[SEE PROFILE](#)

Photoenhanced Degradation of Methylene Blue on Cospattered M:TiO₂ (M = Au, Ag, Cu) Nanocomposite Systems: A Comparative Study

Parvaneh Sangpour,^{†,‡} Fatemeh Hashemi,[†] and Alireza Z. Moshfegh*,^{†,§}

Department of Physics, Sharif University of Technology, P.O. Box 11155-9161, Tehran, Iran, Material and Energy Research Center, P.O. Box 14155-4777, Tehran, Iran, and Institute for Nanoscience and Nanotechnology, Sharif University of Technology, P.O. Box 14588-8969, Tehran, Iran

Received: November 2, 2009; Revised Manuscript Received: June 16, 2010

Titania thin film system containing noble metallic nanoparticles such as Au, Ag, and Cu have been prepared by utilizing radio frequency reactive magnetron cospattering method. The structural and morphological properties of the thin films were characterized by X-ray diffraction (XRD) and atomic force microscopy (AFM). Surface chemical composition of the films was determined by X-ray photoelectron spectroscopy (XPS). Optical properties of the TiO₂ annealed films containing Au, Ag, and Cu metallic nanoparticles were investigated by UV–visible spectrophotometry showing surface plasmon resonance of the metals. The photocatalytic activity of all synthesized samples annealed at 600 °C in an Ar + H₂(80 + 20%) environment was evaluated by measuring the rate of photodegradation reaction of methylene blue (MB) under similar conditions in the presence of UV and visible light irradiation. The Au:TiO₂ and Cu:TiO₂ thin film systems significantly enhanced photodecomposition of MB resulting in 80 and 90% of its initial concentration after 200 min photoirradiation, respectively. The increase in the surface roughness measured by AFM observation and the presence of the Ti³⁺ oxygen vacancy in the photoirradiated thin films were found responsible for the enhancement of the MB photodegradation reaction. The photoenhancement of the studied was determined in the following order: Cu:TiO₂ > Au:TiO₂ > Ag:TiO₂ > TiO₂.

1. Introduction

Photocatalysis is one of the main chemical routes for destruction of environmental toxic pollutants. Metal oxide semiconductor heterogeneous photocatalysts are playing an important role in many industrial and technological processes, in both environmental and biomedical application.^{1–4} Among many metal oxides, TiO₂ possesses excellent photocatalysis. When TiO₂ catalysts are subjected to UV–vis irradiation with photons of energy equal or higher than their band gap (3.2 eV),⁵ the generated electron–hole pairs can induce formation of reactive oxygen species (ROS), such as ·OH and O²⁻, that are directly involved in the oxidation processes leading to degradation of organic pollutants such as methylene blue (MB).⁶

Nanosized noble metal particles or nanoparticles have received extensive attention due to their important potential applications.⁷ Very recently, properties, preparation methods, and applications of nanoparticle catalyst are extensively described and reviewed.⁸ Many researchers have demonstrated that the addition of noble metals, such as Pt,⁹ Pd,¹⁰ Au,¹¹ Ag,¹² and metal oxide semiconductors¹³ to titania, can effectively enhance the degradation efficiency of photocatalytic reactions. This is because they act as an electron trap promoting interfacial charge transfer processes in the composite systems. As a result, more photoinduced holes will have opportunity to participate in the oxidation reactions on the surface. However, with further loadings of noble metal particles, the chance of recombination

of photoinduced electrons and holes will increase leading to reduction in the rate of a decomposition reaction.¹⁴

MB is a heterocyclic aromatic chemical compound with molecular formula C₁₆H₁₈ClN₃S. It has many uses in a range of different fields, such as biology and chemistry. It appears as a solid, odorless, dark-green powder that yields a blue solution when dissolved in water at room temperature. This dye is stable and incompatible with bases, reducing agents, and strong oxidizing agents. During a chemical or biological reaction pathway, these dye compounds not only deplete the dissolved oxygen in water bodies but also release some toxic compounds to endanger aquatic life.^{15,16} MB has been reported to be photobleached, demethylated, and photodegraded under visible light irradiation on a proper catalyst.^{12,17} Some of the nanosystems such as TiO₂ film or its nanoparticle catalysts can decompose MB to safe solution under UV irradiation.

It is well established that metal nanoparticles doping in TiO₂ can influence the intrinsic properties of the semiconductor catalyst and extend its photoresponse into the visible. For example, Zang et al.¹⁸ showed that doping of TiO₂ with noble metal ions, including Pt, Ir, Rh, Au, Pd, Co, and Ni, makes the catalyst absorb light in the visible region of the spectrum.¹⁹ A recent study of Paola and co-workers²⁰ showed that inclusion of transition metal ions increased photocatalytic activity of TiO₂ under UV irradiation. A summary list of very recent studies on photodegradation of MB by different photocatalytic nanosystems prepared by different physical and chemical methods is listed in Table 1. To the best of our knowledge, this is the first comprehensive and comparative report on growth, characterization, and photocatalytic activity on the cospattered M:TiO₂ (M = Au, Cu, Ag) nanocomposite systems during MB degradation reaction.

* To whom correspondence should be addressed. E-mail: moshfegh@sharif.edu.

[†] Department of Physics, Sharif University of Technology.

[‡] Material and Energy Research Center.

[§] Institute for Nanoscience and Nanotechnology, Sharif University of Technology.

TABLE 1: List of Recently Investigated Photocatalytic Activity of Nanosystems for MB Degradation under UV Irradiation Studied by Researchers

systems	preparation method	decomposition (%)	irradiation time (min)	ref
Ag@TiO ₂	sol-gel	55	30	32
Au-TiO ₂	sol-gel	80	600	11
Cu-TiO ₂	solution combustion	60	120	13
Fe-TiO ₂	hydrothermal method	18	180	41
Cu-TiO ₂	sol-gel	67	300	38
Cu-TiO ₂	reactive sputtering	52	90	37
Ag-ZnO	spray flame reactor	100	120	39
V ₂ O ₅ -TiO ₂	impregnation	60	200	40
Ag-ZnO	sol-gel	43	240	42

In this paper, we have investigated the synthesis and effect of addition of metal nanoparticles such as Au, Ag, and Cu into TiO₂-based system matrices as compared to pure TiO₂ films during the photocatalytic degradation reaction of MB in the presence of UV and visible irradiation. In addition, we have also studied the effect of surface roughness and the system work function on photocatalytic activity of metallic TiO₂ and its nanoparticle-doped systems relative to pure TiO₂ thin film.

2. Experimental Section

2.1. Catalyst Preparation. Transparent TiO₂ thin films containing noble metal nanoparticles were deposited on pre-cleaned quartz substrates with dimension of 5 × 15 mm² by utilizing the RF reactive magnetron cosputtering technique. The deposition chamber was evacuated to a base pressure of about 4 × 10⁻⁷ Torr. The distance between target and substrate was about 70 mm. A quartz crystal oscillator was calibrated and used to monitor in situ growth for the desired film thickness. A schematic arrangement with some geometrical details of the sputtering system can be found elsewhere.²¹ Two similar pieces of the desired individual metal (Au, Ag, or Cu) with same diameter (0.2 mm) and similar length (1 mm) were placed symmetrically on a Ti target with 50 mm in diameter. Prior to each deposition, a presputtering process was performed for about 1 min. Co-sputtering of M:TiO₂ system was carried out by applying 100 W of RF power at a pressure of 20 mTorr in an Ar + O₂ (60 + 40%) discharge gas. The “as-deposited” M:TiO₂ nanocomposite films with a thickness of about 100 nm were annealed at 600 °C in a reducing Ar + H₂ (80 + 20%) environment for 1 h. It is noticeable that molar concentrations of Au, Ag, and Cu nanoparticles in their matrix was about 2.7% and considered the same amount for the three systems. A similar molar concentration of the metallic particles was measured by X-ray photoelectron spectroscopy (XPS) for the three nanocomposite M:TiO₂ systems.

2.2. Catalyst Characterization. Optical absorption measurements of the prepared samples were performed in a range of 300–1100 nm using a UV–visible spectrophotometer with resolution of 1 nm for observing surface plasmon resonance band to confirm formation of the metal nanoparticles in the TiO₂ matrix. Surface feature and topography of the films were studied by atomic force microscopy (AFM) in air with a silicon tip of 10 nm radius in contact mode. XPS with Al K α anode at energy of 1486.6 eV was employed to investigate the surface atomic composition, chemical state, and stoichiometry of the titania thin films containing the metal nanoparticles. All binding energy values were determined by calibration and fixing the C(1s) core level peak to 285.0 eV. Crystallinity and phase orientations of the deposited TiO₂ nanocomposite films were determined by

X-ray diffraction (XRD) technique measured with Cu K α radiation source ($\lambda = 1.54 \text{ \AA}$) under the accelerating voltage of 40 kV and the current of 40 mA with a normal θ –2 θ scan.

2.3. Photocatalytic Activity. Photocatalytic performance of each synthesized thin film sample was determined by evaluating the rate of the degradation reaction of MB under similar conditions. For measuring the photocatalytic reaction rate, the annealed M:TiO₂ thin film catalyst were dipped into 20 mL of MB aqueous solution with a concentration of 2 ppm. It was first kept in the dark place for complete absorption of MB on the surface as a reference point. Then they were irradiated by a UV lamp ($\lambda \geq 254 \text{ nm}$, 6 W, Philips, Holland). A 500-W halogen lamp as the visible light source was also used for investigating the activity of the M:TiO₂ nanocatalysts under the similar conditions applied for the UV irradiation experiments. A cutoff filter was applied to remove wavelengths below 420 nm to ensure complete irradiation by visible light. The concentration of MB in the solution was measured as a function of irradiation time by using Beer–Lamberts Law.¹²

In consideration of M:TiO₂ thin films as multicomponent systems, the absorbance of the film is equal to the sum of each component existed in the film and expressed as follows¹⁷

$$A(t, \lambda) = \Sigma [X] \epsilon_x^\lambda L \quad (1)$$

where $A(t, \lambda)$ is the absorbance at the UV irradiation at time t and at wavelength λ , $[X]$ is the molar concentration of MB, ϵ_x^λ is the molar absorption coefficient of X at wavelength λ , and L is the optical path length. From eq 1, we have measured maximum absorption for each X . The wavelength of the absorption maximum for MB is about 664 nm. Also, we have drawn the absorption of MB as a function of its initial concentration (not shown here). The plotted curve shows a linear behavior and the slope of the line is computed about 0.1985. The obtained constant slope representing value ($\epsilon_x^\lambda L$), and it was used to measure absorption of MB in different irradiation time.

The photocatalytic activity of the samples was investigated in both the absence and presence of the catalysts. Since the wavelength of absorbance maximum of methylene blue (λ_{\max}) was found at 664 nm, the photometric analysis of the all photocatalyst samples before and after irradiation can be used by measuring degradation efficiency of MB ($D\%$) defined by the following expression:²²

$$D\% = 100 \times \frac{C_0 - C}{C_0} \quad (2)$$

where C_0 is the initial concentration of MB and C is the concentration of MB after irradiation of the samples in desired time interval.

The degree of absorbance of the samples was measured by the UV–vis spectrophotometer described in experimental section. The decrease of absorbance for the samples at λ_{\max} after irradiation in a desired time interval represents the rate of decolorization (Figure 1) and, therefore, photodegradation efficiency of the MB as well as the activity of the photocatalysts containing nanoparticles. In addition, we have also measured the rate of MB degradation reaction (k) at a given time by using the following equation

$$\ln \frac{C_0}{C} = kt \quad (3)$$

To obtain and optimize MB degradation efficiency and the reaction rate, different synthesized TiO_2 catalyst thin films containing a desired metal nanoparticle were examined under similar conditions, and the results are presented in the following section. Figure 2 shows the change in absorption spectral when the MB aqueous solution was degraded with the pure TiO_2 photocatalyst film after 200 min. The intensity of the maximum absorption peak was decreased due to the MB photodegradation and is shifted toward blue because of the MB demethylation process. The Beer–Lambert law was also used to determine molar concentrations of the demethylated MB.

3. Results and Discussion

3.1. Optical Properties. UV-vis absorption spectra of TiO_2 thin film catalysts containing Au, Ag and Cu nanoparticles are shown in Figure 2. The results indicate that the maximum absorption peaks of the synthesized nanocomposite thin films, namely, $\text{Ag}:\text{TiO}_2$, $\text{Au}:\text{TiO}_2$, and $\text{Cu}:\text{TiO}_2$ were identified at 424, 552, and 578 nm, respectively. These observed surface plasmon resonance (SPR) peaks indicating formation of metallic nanoparticles in the TiO_2 matrix as also reported by other researchers.^{23,24} It is well established that in metallic nanoparticles such as Au^0 , Cu^0 , and Ag^0 the surface plasmon absorption arises from the collective oscillations of the free conduction band electrons that are induced by the incident electromagnetic radiation. The observation of the SPR band in the visible region of solar spectrum is the first simple measurement to prove formation of metal nanoparticles in a dielectric matrix. It should be noted that the difference in maximum absorption values for the different systems in Figure 2 is due to difference of dielectric constant Cu, Ag, and Au and also the difference in their average nanoparticles size.²⁵ This is because in absorption of metals dispersed in a dielectric matrix two factors, namely, the size of metal nanoparticle and its dielectric constant play an important role in the process. A detailed discussion about the generation of surface plasmon resonance peak can be found elsewhere.²⁶

3.2. AFM Results. Figure 3 shows AFM images of $\text{Au}:\text{TiO}_2$, $\text{Ag}:\text{TiO}_2$, and $\text{Cu}:\text{TiO}_2$ thin films. The average surface roughness of the thin films was calculated by using our statistical data analysis of all the AFM images a proper through software. On the basis of our measurements, the average surface roughness for $\text{Cu}:\text{TiO}_2$, $\text{Au}:\text{TiO}_2$, and $\text{Ag}:\text{TiO}_2$ is about 3, 2.4, and 1.3

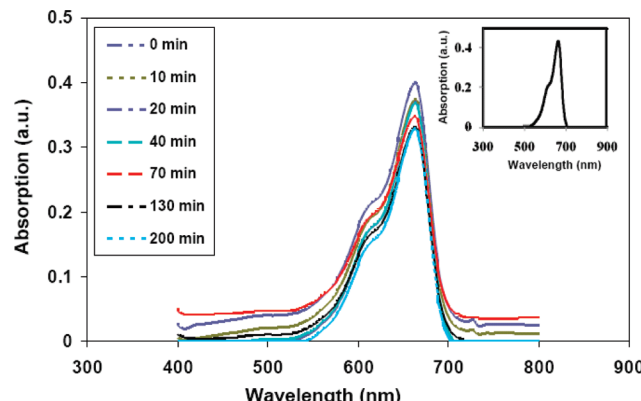


Figure 1. Absorption of an irradiated solution containing initially 2 ppm MB at different UV irradiation time for the pure TiO_2 thin film (0 min is related to placed container in dark). The inset figure is attributed to absorption of 2 ppm MB solution containing glass substrate.

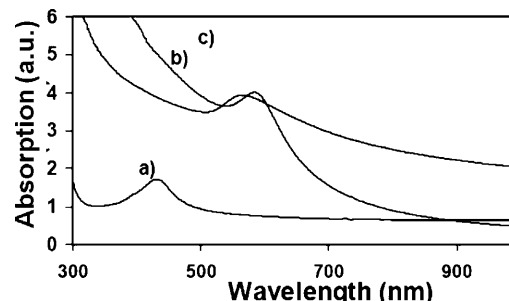


Figure 2. Optical absorption spectra of the annealed ($600\text{ }^\circ\text{C}$) TiO_2 thin films containing different nanoparticles (a) Ag, (b) Au, and (c) Cu.

nm, respectively. Also, beside each AFM images we have drawn a size distribution histogram. These figures show that Cu nanoparticles in TiO_2 matrix have least average size distribution on the surface as compared to other two nanocomposite thin film systems.

3.3. Scanning Electron Microscopy (SEM) Results. Surface morphology and variation of particle size on the surface of the systems were studied by the SEM method. SEM images of the titania films containing gold, silver, and copper nanoparticles have been shown in Figure 4. A uniform distribution of nanoparticles was found on the surface of the films. The observed nanospherical average grain size was estimated of about 90, 50, and 35 nm for $\text{Au}:\text{TiO}_2$, $\text{Ag}:\text{TiO}_2$, and $\text{Cu}:\text{TiO}_2$, respectively.

Our AFM results also confirmed the SEM observations so that the average grain size measured by the two methods was approximately the same for each sample. The AFM image of the films has been shown in Figure 4 indicating that the particlelike features on the surface. It was also seen from AFM images that the distribution of the particles on the surface are uniformly distributed supporting our SEM observation.

3.4. Photocatalytic Activity Results. Figure 5a shows the changes in normalized concentration of MB with irradiation time without using any catalyst. About 12% reduction in C/C_0 was measured under time situation. Figure 5b shows the normalized concentration was degraded by pure and metallic doped TiO_2 thin films after 200 min. Investigation of XRD patterns for the pure TiO_2 thin film showed that the growth of TiO_2 is crystalline with anatase structure. According to XRD analysis, an intense peak at $2\theta = 25.2^\circ$ was observed (not shown here) due to formation of the anatase phase in the all investigated system.

The initial process for photocatalysis of organic compounds by TiO_2 is the generation of $e^- - h^+$ pairs. The generated holes (h^+) react with H_2O and OH^- groups adsorbed on the surface of TiO_2 to produce hydroxyl radicals,²⁷ and the electrons (e^-) are attracted to the metal particle due to the difference in the work functions between TiO_2 and metal nanoparticles, thus preventing the $e^- - h^+$ recombination process (see eqs 46).²⁷ The addition of metal clusters in the TiO_2 thin films is expected to improve the charge separation by acting as an electron sink, and consequently it increases the number of electrons reaching the surface for reaction to take place.^{28,29} Furthermore, more catalyst surfaces will be covered by the additional noble metal, which will lead to a declined yield of photoinduced-electrons and holes.²⁸

Figure 5b shows the degradation of MB with irradiation time by the different photocatalysts. The first important observation was that all photocatalysts had attained conversion within the monitored reaction period (200 min). The addition of different metals to TiO_2 thin film did not provide the same behavior in

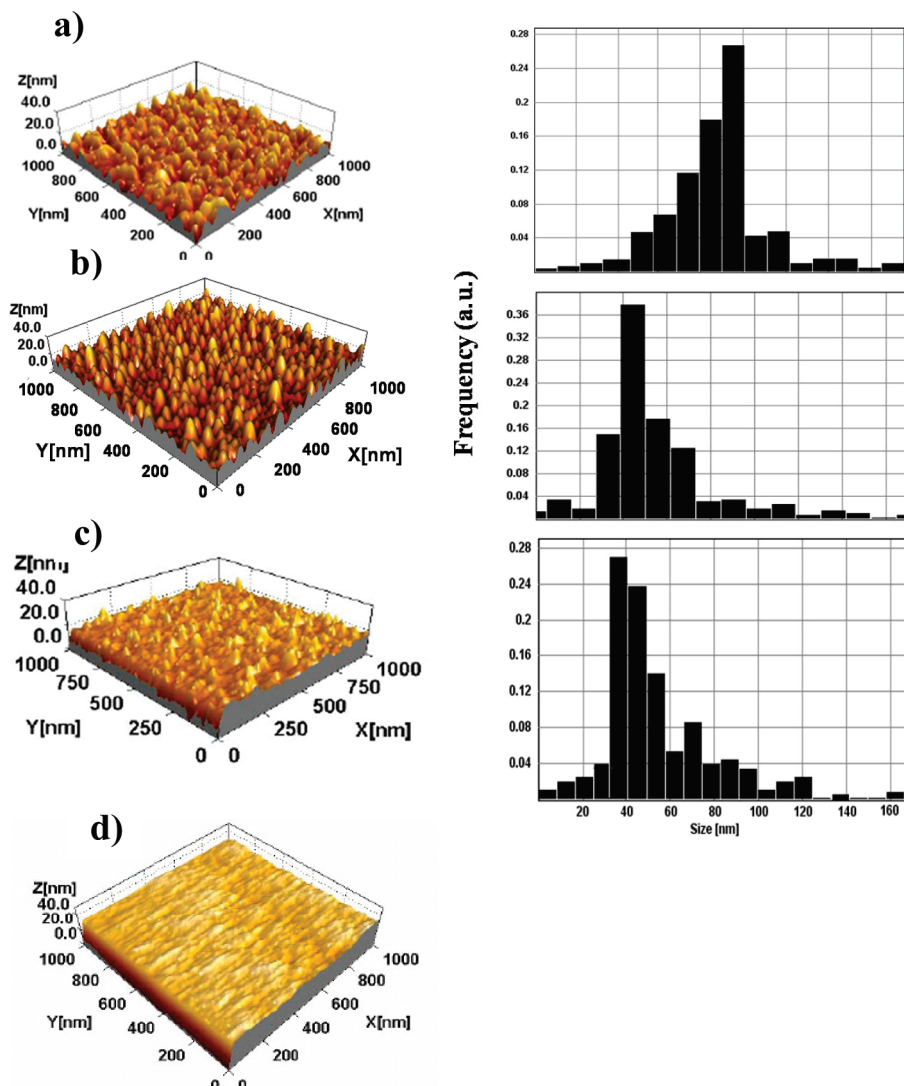


Figure 3. 3D AFM images ($1 \times 1 \mu\text{m}^2$) of the annealed (600°C) TiO_2 thin films containing (a) Au, (b) Ag, and (c) Cu nanoparticles. (d) AFM image of the pure annealed TiO_2 thin film at 600°C .

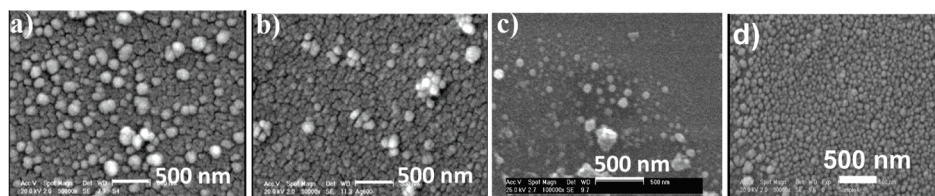
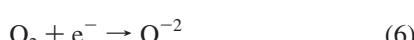
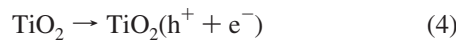


Figure 4. SEM images of the annealed (600°C) TiO_2 thin films containing (a) Au, (b) Ag, and (c) Cu nanoparticles. (d) SEM image of the pure annealed TiO_2 thin film at 600°C .

photocatalytic reaction. The following steps occur during the photocatalytic reduction of the metals in the presence of TiO_2 media.³⁰



Equation 4 represents the generation of electrons in conduction band and holes in valence band, and the oxidation of water

is also occurred by the generated holes as described in eq 5. Finally, MB molecules are attacked by the highly oxidizing OH^\cdot radicals resulting in its decomposition process as shown below³¹



The TiO_2 thin films act as catalysts for degradation of MB (Figure 6b). After 200 min of photoirradiation, about 40% of MB was decomposed. The efficiency of the photodegradation is enhanced by doping metal nanoparticles. In the case of the Au: TiO_2 composite thin film catalyst, about 80% of the MB solution was decomposed after 200 min UV irradiation.

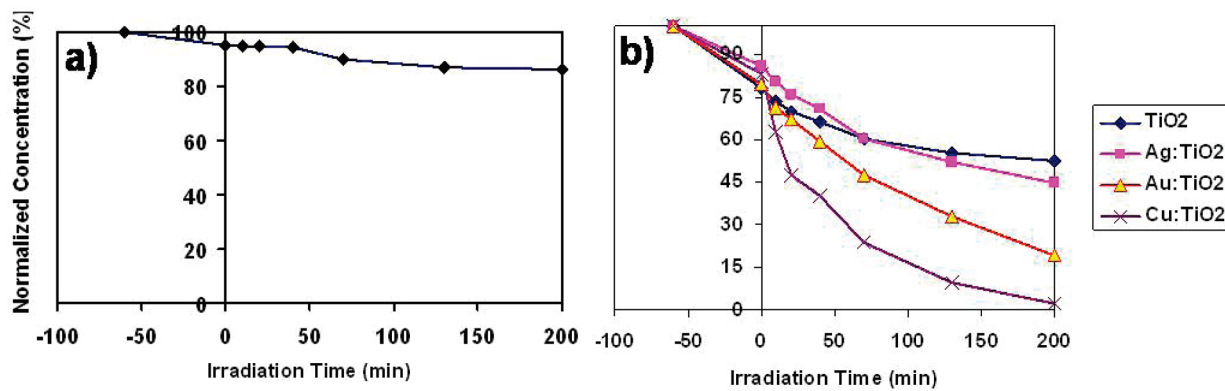


Figure 5. The variation of normalized C/C_0 of MB concentration as a function of UV irradiation time (a) without any catalyst nanoparticles. (b) TiO_2 thin films containing Au, Ag, and Cu nanoparticles annealed at 600 °C.

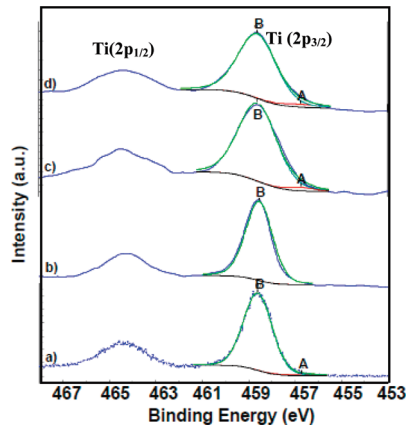


Figure 6. XPS spectra of the Ti(2p) core level for the 600 °C annealed TiO_2 thin films containing different nanoparticles (a) pure TiO_2 , (b) Au: TiO_2 , (c) Ag: TiO_2 , (d) Cu: TiO_2 . A and B peaks are related to Ti^{3+} and Ti^{4+} surface chemical states, respectively.

TABLE 2: Summary of Deconvolution of XPS Spectra of Pure TiO_2 Thin Films and TiO_2 Thin Films Containing Metallic Nanoparticles

system	Ti^{4+} (%)	Ti^{3+} (%)	fwhm	baseline broadening (eV)
TiO_2	98.7	1.3	1.47	5.8
Au: TiO_2	99.9	0.1	1.82	5.5
Ag: TiO_2	96.9	3.1	1.94	5.7
Cu: TiO_2	95.5	4.5	1.94	5.9

However, photocatalytic activity is markedly enhanced in the presence of the TiO_2 , but we believe that the Au nanoparticles inhibit the recombination of charge carriers by electron capture. Thus more holes are available to produce hydroxyl radicals resulting in enhancement of the photodegradation process. About 50% of MB was degraded by using Ag: TiO_2 . Doping TiO_2 thin film by Cu nanoparticles resulted in further enhancement of the photocatalytic activity of the film yielding about 96% of MB degraded under similar reaction conditions. Ag: TiO_2 thin films have a better decomposition efficiency as compared with TiO_2 thin films (see Table 2). This is because if TiO_2 thin films are not connected with Ag nanoparticles then electrons will accumulate on those metal particles without adsorbed oxygen, causing charge recombination and lower quantum efficiency.³² At the same time, electrons of Ag nanoparticles, when irradiated with the light, are excited and transformed to adsorbed oxygen forming O^{2-} ions. The Ag nanoparticles are consequently oxidized by O^{2-} to colorless Ag^+ ions.³² In presence of TiO_2

these Ag^+ ions are reduced by the excited electrons and Ag nanoparticles are reformed.

The measured differences in photocatalytic activities of TiO_2 thin films containing various metal nanoparticles can be explained as the effect of difference in work functions between the noble metal and the semiconductor.³³ Generally, when two materials with different work function contact each other, the Schottky barrier will be formed, and electrons will transfer from the material with low work function to the material with high work function. The work function of noble metals, such as Pt (5.64 eV), Pd (5.12 eV), Au (5.1 eV), Ag (4.2 eV), and Cu (4.93),³³ is higher than TiO_2 (4.2 eV).³³ When metal-modified TiO_2 nanocomposite films are excited by light irradiation, a portion of photoinduced electrons from TiO_2 will transport to the metal particles and will be scavenged by the electron acceptor, commonly the O_2 species³⁶ absorbed on the surface. Under these conditions, Au: TiO_2 thin film shows more effective electron-acceptor properties due to the larger work function of Au in comparison with Ag and Cu. Although Cu has a lower work function as compared with Au, but Cu: TiO_2 thin films showed a higher photodegradation as compared to Au: TiO_2 and Ag: TiO_2 systems (Figure 5). This behavior was also observed by Li et al.³⁵ for photocatalytic activity of Ag as compared to Pd (during degradation of MB).

To understand the reason behind the difference in photocatalytic activity of the investigated nanocomposite systems, we have studied XPS data for all the systems. It is necessary to note that for analyzing XPS data we have used software SDP (4v), and all binding energy values were determined by calibration and fixing the C(1s) core level peak to 285.0 eV. All of the peaks were deconvoluted using SDP software (version 4.1) with 80% Gaussian–20% Lorentzian peak fitting. Figure 6 shows XPS spectrum of Ti(2p) peak for the titania thin films containing metal nanoparticles and Pure TiO_2 thin films. It consists of the Ti(2p3/2) peak at 458.8 eV and the Ti(2p1/2) peak at 464.5 eV. These energy values are close to those reported in the literature for the TiO_2 films at 458.9 and 464.6 eV for Ti(2p3/2) and Ti(2p1/2), respectively. It is necessary to note that the core level binding energy of about 456.7 eV and 458.5 eV are related to Ti_2O_3 and TiO_2 , respectively. The summarized results of XPS analysis were reported in Table 2. On the basis of XPS analysis, in the first step, formation of the TiO_2 film is confirmed. In addition, XPS measurement (Figure 6) indicated that for the TiO_2 thin films containing Cu nanoparticles about 5% of Ti(2p) is in Ti_2O_3 chemical state, resulting in formation of Ti^{3+} on the surface. Thus, it shows that there is a deficiency of oxygen on the surface and an increase of O^{2-} anion that prevents recombination of electron–hole pair on the

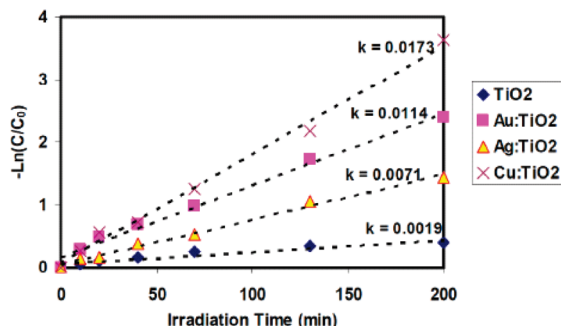
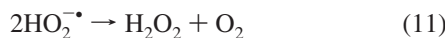
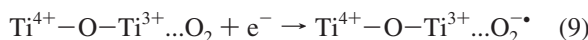
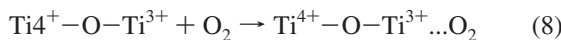


Figure 7. The variation of normalized $-\ln C/C_0$ MB concentration as a function of UV light irradiation time for TiO_2 thin films containing Au, Ag, and Cu nanoparticles annealed at 600°C .

surface.³⁴ Therefore, these positive effects resulted in increase in the rate of degradation reaction rate on the Cu:TiO₂ thin film as compared to other studied systems. On the basis of our data analysis the following reactions can occur in presence of Ti³⁺ during the process



The role of produced OH[·] radicals in the above reaction is attacking MB molecules to open the central aromatic rings via multistep intermediate reactions which result in an increase in the rate of MB decomposition process (eq 3); consequently, we have a highly degraded concentration of MB by using Cu:TiO₂ nanocomposite.³¹ In addition, by consideration of the rate comparison, it is worthy of noting that surface area of all of the investigated system is similar, but their surface roughness, which plays a more important role in the photocatalytic process, is different. On the basis of AFM observation, Cu:TiO₂ nanocomposite has a larger surface roughness as compared with other investigated systems and then has the most photocatalytic activity. Jung et al.²⁹ reported that the surface roughness improves photocatalytic activity (degradation of MB on TiO₂ matrix), which is in good agreement with our results.

Figure 7 shows the rate of MB degradation on various synthesized thin films as a function of photoirradiation time. It is evident, by adding metallic nanoparticles, that the rate of degradation reaction was increased. A summary of our results for different metal nanoparticles dispersed in TiO₂ thin films is listed in Table 3.

Figure 8 shows the normalized concentration was degraded by pure and metal-doped TiO₂ thin films after 240 min under visible light irradiation. As seen from Figure 8, visible light can degrade MB by using pure TiO₂ thin films and metal-doped TiO₂. The time during the degradation is longer than using UV irradiation.

Figure 9 shows the variation of normalized $-\ln C/C_0$ of MB concentration as a function of visible light irradiation, respec-

TABLE 3: Summary of Parameters Affecting the Rate of Photodegradation of MB by Different Samples under UV Light Irradiation

system	r_{rms} (nm)	work function (eV)	$k (\text{min}^{-1})$ $\times 10^{-3}$ UV irradiation	$k (\text{min}^{-1})$ $\times 10^{-3}$ visible irradiation	D (%)
TiO ₂	1.2	4.2	1.9	1.5	40
Au:TiO ₂	2.4	5.1	11.4	6.5	50
Ag:TiO ₂	1.3	4.6	7.1	4	75
Cu:TiO ₂	3.0	4.9	17.3	5.5	90

tively. As shown in the Figure 9, the presence of metal nanoparticles in the TiO₂ matrix leads to exciting the electron–hole pair by visible light, while no significant change in the rate of MB photodegradation is observed when pure TiO₂ layers were used as catalyst under UV and visible photoirradiation. This is because the band gap energy of the TiO₂ layers is about 3.2 eV, so no electron–hole pairs, which are necessary for photocatalytic reactions, are generated under visible light irradiation. In contrast, nanocomposite systems containing metallic nanoparticles show a better photoactivity under visible light due to their lower band gap energy as compared to pure TiO₂ thin films. Because of this relatively narrow band gap energy, they can be excited by visible illumination; therefore, electron–hole pairs are generated by the grown composite layers even under visible light. But, it is noticeable that the time needed for photocatalyst reaction by visible light is longer than for UV irradiation. The behavior of thin films containing nanoparticles under visible light is similar to UV irradiation, which the films containing Cu nanoparticles have most degradation during 240 min visible photoirradiation as compared to the other TiO₂-doped nanocomposite systems. The photocatalytic reaction rate was in highest value for Cu:TiO₂ (see Figure 9) as compared to other system determined.

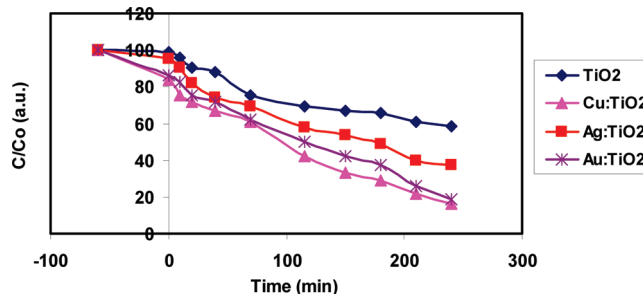


Figure 8. The variation of normalized C/C_0 of MB concentration as a function of visible irradiation of TiO_2 thin films and TiO_2 thin films containing Au, Ag, and Cu nanoparticles annealed at 600°C .

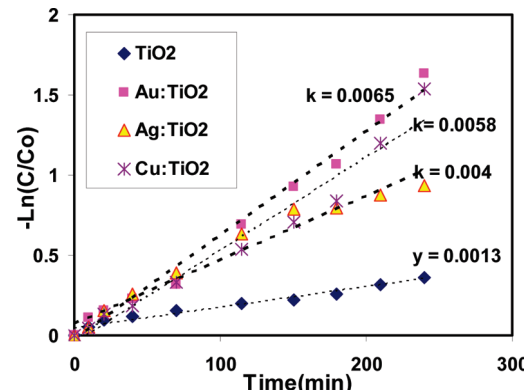


Figure 9. The variation of normalized $-\ln C/C_0$ of MB concentration as a function of visible light irradiation time for TiO_2 thin films containing Au, Ag, and Cu nanoparticles annealed at 600°C .

4. Conclusions

We have investigated the photocatalytic activity of the TiO₂ thin films containing different metallic nanoparticles (Au, Ag, and Cu) prepared by RF magnetron cosputtering method as compared to pure TiO₂ thin films. It was found that Au:TiO₂ and Cu:TiO₂ thin films provide a higher catalytic performance in MB degradation reaction under UV and visible photoirradiation. The enhancement was found due to presence of metallic nanoparticles which inhibit the charge carrier recombination by electron capture resulting in more holes formation to produce hydroxyl radicals leading to increase in the rate MB photodegradation reaction. In addition, XPS measurement indicated the presence of a Ti³⁺ chemical state for the TiO₂ thin films containing Cu nanoparticles showing formation of Ti₂O₃ phase on the surface. It was determined that deficiency of O₂ on the surface and increase of O²⁻ anion preventing recombination of electron–hole pair on the surface resulting in increase of degradation reaction rate on the film. It was also found that the average surface roughness of the films further improves photocatalytic performance during the MB degradation reaction.

Acknowledgment. The authors would like to thank Research and Technology Council of Sharif University of Technology for financial support of the project. Assistance of Mr. Raffie for XPS and Mrs. Vaseghinia for AFM measurements is greatly acknowledged.

References and Notes

- (1) Kiwi, J.; Pulgarine, C. M.; Gratzel, P. P. *Appl. Catal., B* **1993**, *3*, 85.
- (2) Hoffman, M. R.; Martin, S. T.; Choi, W.; Bahnemann, D. W. *Chem. Rev.* **1995**, *95*, 69.
- (3) Kastner, J. R.; Thompson, D. N.; Cherry Kaster, R. S. *Enzyme Microb. Technol.* **1999**, *24*, 104.
- (4) Martha Miller, J.; Grant Allen, D. *J. Chem. Eng.* **2005**, *113*, 197.
- (5) Chang, C. Ch.; Lin, C. K.; Chan, C. Ch.; Sh. Hsu, Ch.; Chen, Ch. Y. *Thin Solid Films.* **2006**, *494*, 274.
- (6) Zhu, J.; Ren, J.; Huo, Y.; Bian, Zh.; Li, H. *J. Phys. Chem. C* **2007**, *111* (51), 18965.
- (7) Ismail, Adel A.; Bahnemann, D. W.; Bannat, I.; Wark, M. *J. Phys. Chem. C* **2009**, *113* (17), 7429.
- (8) Moshfegh, A. Z. *J. Phys. D: Appl. Phys.* 2009, 42 in press.
- (9) Li, X. Z.; Li, F. B. *Environ. Sci. Technol.* **2001**, *35*, 2381.
- (10) You, X.; Chen, F.; Zhang, J.; Anpo, M. *Catal. Lett.* **2005**, *102*, 247.
- (11) Uddin, M. J.; Cesano, F.; Scarano, D.; Bonino, F.; Agostini, G.; Spoto, G.; Bordiga, S.; Zecchina, A. *J. Photochem. Photobiol. A: Chem.* **2008**, *199*, 64.
- (12) Senthilkumaar, S.; Porkodi, K.; Gomathi, R.; Geetha Maheswari, A.; Manonmani, N. *Dyes Pigments* **2006**, *69*, 22.
- (13) Xu, Y.; Liang, D.; Liu, M.; Liu, D. *Mater. Res. Bull.* **2008**, *43*, 3474.
- (14) Kowalska, E.; Remita, H.; Colbeau-Justin, C.; Hupka, J.; Belloni, J. *J. Phys. Chem. C* **2008**, *112* (4), 1124.
- (15) Obata, H.; Koizumi, M. *Bull. Chem. Soc. Jpn.* **1957**, *30*, 142.
- (16) Obata, H.; Kogasaka, K.; Koizumi, M. *Bull. Chem. Soc. Jpn.* **1959**, *32*, 125.
- (17) Yogi, Ch.; Kojima, K.; Wada, N.; Tokumoto, H.; Takai, T.; Mizoguchi, T.; Tamiaki, H. *Thin Solid Films* **2008**, *516*, 5881.
- (18) Zang, L.; Macyk, W.; Lange, C.; Maier, W. F.; Antonius, C.; Meissner, D.; Kisch, H. *J. Chem. Eur.* **2000**, *6*, 379.
- (19) Subramanian, V.; Wolf, E.; Kamat, P. V. *Langmuir* **2003**, *19*, 469.
- (20) Paola, D.; Marci, A.; Palmisano, G.; Schiavello, L.; Uosaki, M.; Ikeda, K.; Ohtani, S. *J. Phys. Chem. B* **2002**, *106*, 637.
- (21) Moshfegh, A. Z.; Akhavan, O. *J. Phys. D: Appl. Phys.* **2001**, *34*, 2103.
- (22) Pouretedala, H. R.; Norozi, A.; Keshavarz, M. H.; Semnani, A. *J. Hazard. Mater.* **2009**, *162*, 674.
- (23) Link, S.; Wang, Z. L.; El-Sayed, M. A. *J. Phys. Chem. B* **1999**, *103*, 3529.
- (24) Lance Kelly, K.; Yamashita, K. *J. Phys. Chem. B* **2006**, *110* (15), 7743.
- (25) Babapour, A.; Akhavan, O.; Azimrad, R.; Moshfegh, A. Z. *Nanotechnol.* **2006**, *17*, 763.
- (26) Noguez, C. *Opt. Mater.* **2005**, *27*, 1204.
- (27) Syoufian, A.; Nakashima, K. *J. Colloid Interface Sci.* **2008**, *317*, 507.
- (28) Sa, J.; Fernandez-Garcia, M.; Anderson, J. A. *Catal. Commun.* **2008**, *9*, 1991.
- (29) Jung, J. M.; Wang, M. E.; Kim, J.; Park, Ch.; Hahn, S. H. *Appl. Catal. B: Environ.* **2008**, *84*, 389.
- (30) Aarthi, T.; Madras, G. *Catal. Commun.* **2008**, *9*, 630.
- (31) Houas, A.; Lachheb, H.; Ksibi, M.; Elaloui, E.; Guillard, C.; Herrmann, J. M. *Appl. Catal. B: Environ.* **2001**, *31*, 145.
- (32) Sobana, N.; Selvam, K.; Swaminathan, M. *Sep. Purif. Technol.* **2008**, *62*, 648.
- (33) Yang Teoh, W. *Flame spray synthesis of catalyst nanoparticles for photocatalytic mineralization of organics*; University of New South Wales, 2007.
- (34) Lee, S. H. *Photocatalytic nanocomposites based on TiO₂ and carbon nanotubes*; University of Florida, 2004.
- (35) Li, X.; Liu, T. M.; Fan, Y. Q.; Xu, N. P. *Thin Solid Films* **2008**, *516*, 7282.
- (36) Liu, W.; Chen, Y.; Kou, G.; Xu, T.; Sun, D. *Wear* **2003**, *254*, 994.
- (37) Zhang, W.; Li, Y.; Zhu, Sh.; Wang, F. *Catal. Today* **2004**, *93*, 589.
- (38) Xin, B.; Wang, P.; Ding, D.; Liu, J.; Ren, Z.; Fu, H. *Appl. Surf. Sci.* **2008**, *254*, 2569.
- (39) Wang, R.; Xin, J. H.; Yang, Y.; Liu, H.; Xu, L.; Hu, J. *Appl. Surf. Sci.* **2004**, *227*, 312.
- (40) Mokhtar Mohamed, M.; Al-Esaimi, M. *J. Mol. Catal. A* **2006**, *255*, 53.
- (41) Li, Zh.; Shen, W.; He, W.; Zu, X. *J. Hazard. Mater.* **2008**, *155*, 590.
- (42) Zheng, Y.; Chen, Ch.; Zhan, Y.; Lin, X.; Zheng, Q.; Wei, K.; Zhu, J. *J. Phys. Chem. C* **2008**, *112* (29), 10773.

JP910454R